ON THE ROLE OF THE RUNNING COUPLING CONSTANT IN A QUARK MODEL ANALYSIS OF T-ODD TMDs.

A. COURTOY

Istituto Nazionale di Fisica Nucleare-Sezione di Pavia, Via Bassi 6
27100 Pavia, Italy
aurore.courtoy@pv.infn.it

We revisit the standard procedure to match non-perturbative models to perturbative QCD, using experimental data. The strong coupling constant plays a central role in the QCD evolution of parton densities. We will extend this procedure with a non-perturbative generalization of the QCD running coupling and use this new development to understand why perturbative treatments are working reasonably well in the context of hadronic models. Vice versa, this new procedure broadens the ways of analyzing the freezing of the running coupling constant.

Keywords: hadronic models; coupling constant; non-perturbative.

PACS numbers: 12.38 Aw, 12.38 Bx, 12.39 Ba, 14.20 Dh

1. Parton Distributions and the Hadronic Scale

The internal structure of the strongly interacting particles remains veiled. It is still a challenge to describe consistently the dynamics of scattering processes and hadronic structure at moderate energy scales. Because at such a scale a hadronic representation takes over the partonic description, it is called *the hadronic scale.* The hadronic scale is peculiar to each hadronic representation.

A way of connecting the perturbative and non-perturbative worlds has traditionally been through the study of Parton Distribution Functions (PDFs): Deep Inelastic processes are such that they enable us to look with a good resolution inside the hadron and allow us to resolve the very short distances, i.e. small configurations of quarks and gluons. At short distances, this part of the process is described through perturbative QCD. A resolution of such short distances is obtained with the help of non-strongly interacting probes. Such a probe, typically a photon, is provided by hard reactions. In that scheme, the PDFs reflect how the target reacts to the probe, or how the quarks and gluons are distributed inside the target. The insight into the structure of hadrons is reached at that stage: the large virtuality of the photon, Q^2, involved in such processes allows for the factorization of the hard (perturbative) and soft (non-perturbative) contributions in their amplitudes. Hence, the virtuality

2   *A. Courtoy*

of the photon introduces another scale, i.e. *the factorization scale.*

The evaluation of PDFs is guided by a standard scheme, set up in valuable litterature of the 90s [1, 2, 3]. This scheme runs in 3 main steps. First, we either build models consistent with QCD in a moderate energy range, typically the hadronic scale; or we use effective theories of QCD for the description of hadrons at the same energy range. Second, PDFs are evaluated in these models, giving a description of the Bjorken-x dependence of the distribution. Third, the scale dependence of these distributions is studied. The last step allows to bring the moderate energy description of hadrons to the factorization scale, thanks to the QCD evolution equations. In these proceedings, we will focus on this third step: how to match non-perturbative models to perturbative QCD, using experimental data.

The hadronic scale is defined at a point where the partonic content of the model, defined through the second moment of the parton distribution, is known. For instance, the CTEQ parameterization gives [a]

$$\left\langle (u_v + d_v)(Q^2 = 10 \text{GeV}^2)) \right\rangle_{n=2} = 0.36 \quad , \tag{1}$$

with q_v the valence quark distributions and with $\langle q_v(Q^2) \rangle_n = \int_0^1 dx \, x^{n-1} \, q_v(x, Q^2)$. In the extreme case, i.e., when we assume that the partons are pure valence quarks, we evolve downward the second moment until

$$\left\langle (u_v + d_v)(\mu_0^2) \right\rangle_{n=2} = 1 \quad . \tag{2}$$

The hadronic scale is found to be $\mu_0^2 \sim 0.1$ GeV^2.

This standard procedure to fix the hadronic (non-perturbative) scale pushes perturbative QCD to its limit. In effect, the hadronic scale turns out to be of a few hundred MeV^2, where the strong coupling constant has already started approaching its Landau pole. As it will be shown hereafter, the N^{m}LO evolution converges very fast, what justifies the perturbative approach. Consequently, the behaviour of the strong coupling constant plays a central role in the QCD evolution of parton densities. We here extend the standard procedure with the non-perturbative generalization of the QCD running coupling. We justify the perturbative evolution approach by comparing it to the non-perturbative momentum dependence as determined by the phenomenon of the freezing of the coupling constant, and to analyze the consequences of introducing an effective gluon mass [4]. We use this new development to understand why perturbative treatments are working reasonably well in the context of hadronic models.

2. The Running Coupling Constant

In these proceedings, we call perturbative evolution the renormalization group equations (RGE) that follow from an analysis of the theory as a perturbative expansion

---

[a]MSTW gives a similar result.

in Feynman diagrams with m loops leading to logarithmic corrections of the ratio 'momentum invariant to mass scale', i.e. $\left(\alpha_s \log(P^2/M^2)\right)^m$.

The running of the coupling constant is driven by the RGE. In QCD, α_s is defined by renormalization conditions imposed at a large momentum scale where the coupling is small. The running coupling constant is dimensionless, but through dimensional transmutation, the strength of the interaction may be described by a dimensionful parameter. QCD scale, Λ_{QCD}, is then defined as the energy scale where the interaction strength reaches the value 1.

At N^mLO the scale dependence of the coupling constant is given by

$$\frac{d\, a(Q^2)}{d(\ln\, Q^2)} = \beta_{\text{N}^m\text{LO}}(\alpha_s) = \sum_{k=0}^{m} a^{k+2}\beta_k,$$

where $a = \alpha_s/4\pi$. We show here the solution to $k = 2$, i.e., NLO

$$\beta_0 = 11 - \frac{2}{3} n_f \quad , \quad \beta_1 = 102 - \frac{38}{3} n_f \quad ,$$

where n_f stands for the number of effectively massless quark flavors and β_k denote the coefficients of the usual four-dimensional $\overline{MS}$ beta function of QCD. The evolution equations for the coupling constant can be integrated out exactly leading to

$$\ln(Q^2/\Lambda_{\text{LO}}^2) = \frac{1}{\beta_0 a_{\text{LO}}} \quad ,$$

$$\ln(Q^2/\Lambda_{\text{NLO}}^2) = \frac{1}{\beta_0 a_{\text{NLO}}} + \frac{b_1}{\beta_0}\ln(\beta_0 a_{\text{NLO}}) - \frac{b_1}{\beta_0}\ln(1 + b_1 a_{\text{NLO}}) \quad , \tag{3}$$

where $b_k = \beta_k/\beta_0$. These equations, except the first, do not admit closed form solution for the coupling constant, and we have solved them numerically. We show their solution, for the same value of $\Lambda = 250$ MeV, in Fig. 1.
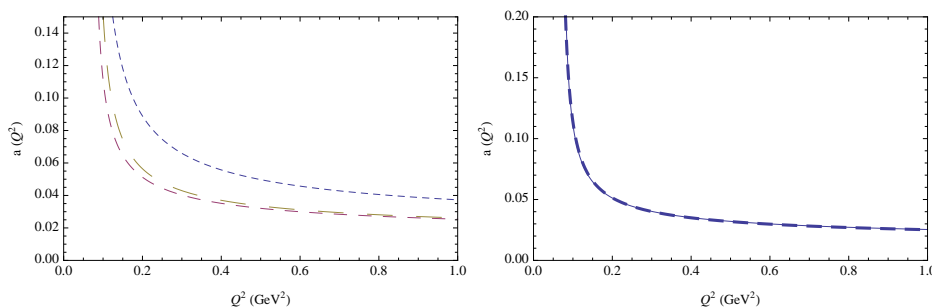

Fig. 1.   The running of the coupling constant. Left: The short dashed curve corresponds to the LO solution, the medium dashed curve to NLO solution and the long dashed curve to the NNLO solution($\Lambda = 250$ MeV). Right: The solid curve represents the NLO solution with $\Lambda = 250$ MeV, while the long dashed curve the NNLO solution with a value of $\Lambda = 235$ MeV.

We see in Fig. 1 (left) that the NLO and NNLO solutions agree quite well even at very low values of Q^2 and in Fig. 1 (right) that they agree very well if we change the value of Λ for the NNLO slightly, confirming the fast convergence of the expansion. This analysis concludes, that even close to the Landau pole, the convergence of the perturbative expansion is quite rapid, specially if we use a different value of Λ to describe the different orders, a feature which comes out from the fitting procedures. *This fast convergence ensures that perturbative evolution can still be used at rather low scales.* However, when entering the non-perturbative regime, other mechanisms take place that influence the QCD evolution. That is what we will call here non-perturbative evolution.

It is well established by now that the QCD running coupling (effective charge) freezes in the deep infrared. This non-perturbative property can be best understood from the point of view of the dynamical gluon mass generation [5, 6, 7, 8]. Even though the gluon is massless at the level of the fundamental QCD Lagrangian, and remains massless to all order in perturbation theory, the non-perturbative QCD dynamics generate an effective, momentum-dependent mass, without affecting the local $SU(3)_c$ invariance, which remains intact. At the level of the Schwinger-Dyson equations the generation of such a mass is associated with the existence of infrared finite solutions for the gluon propagator, i.e. solutions with $\Delta^{-1}(0) > 0$. Such solutions may be fitted by "massive" propagators of the form $\Delta^{-1}(Q^2) = Q^2 + m^2(Q^2)$; $m^2(Q^2)$ is not "hard", but depends non-trivially on the momentum transfer Q^2. One physically motivated possibility, which we shall use in here, is the so called logarithmic mass running, which is defined by

$$m^2(Q^2) = m_0^2 \left[\ln\left(\frac{Q^2 + \rho m_0^2}{\Lambda^2} \right) \bigg/ \ln\left(\frac{\rho m_0^2}{\Lambda^2} \right) \right]^{-1-\gamma}. \tag{4}$$

Note that when $Q^2 \to 0$ one has $m^2(0) = m_0^2$. Even though in principle we do not have any theoretical constraint that would put an upper bound to the value of m_0, phenomenological estimates place it in the range $m_0 \sim \Lambda - 2\Lambda$ [9, 10.] The other parameters were fixed at $\rho \sim 1 - 4$, $(\gamma) = 1/11$ [5, 11, 12]. The (logarithmic) running of m^2, shown in Fig. 2 for two sets of parameters, is associated with the the gauge-invariant non-local condensate of dimension two obtained through the minimization of $\int d^4x (A_\mu)^2$ over all gauge transformations.

The strong coupling constant plays a central role in the evolution of parton densities. The non-perturbative generalization of $\alpha_s(Q^2)$ the QCD running coupling, comes in the form

$$a_{\mathrm{NP}}(Q^2) = \left[\beta_0 \ln\left(\frac{Q^2 + \rho m^2(Q^2)}{\Lambda^2} \right) \right]^{-1}, \tag{5}$$

where we use the same notation as before and NP stands for Non-Perturbative. Note that its zero gluon mass limit leads to the LO perturbative coupling constant momentum dependence. The $m^2(Q^2)$ in the argument of the logarithm
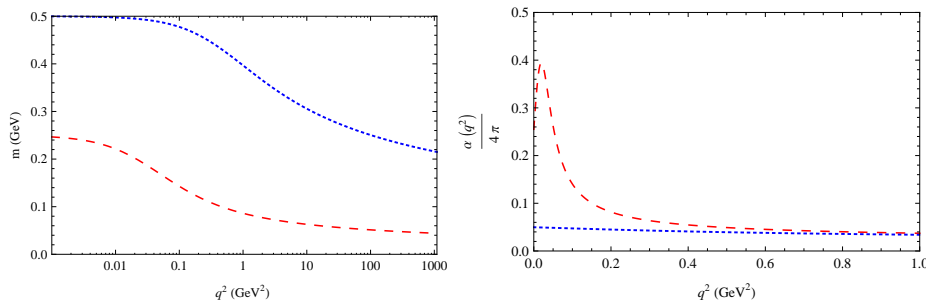
Fig. 2.   Left: The dynamical gluon mass with a logarithmic running for two sets of parameters, the small mass scenario ($\Lambda = 250$ MeV, $m_0 = 250$ MeV, $\rho = 1.5$) is shown by the dashed curve; the high mass scenario ($\Lambda = 250$ MeV, $m_0 = 500$ MeV, $\rho = 2.0$) by the dotted curve. Right: The running of the effective coupling.

tames the Landau pole, and $a(Q^2)$ freezes at a finite value in the IR, namely $a^{-1}(0) = \beta_0 \ln(\rho m^2(0)/\Lambda^2)$ [5, 6, 7] as can be seen in Fig. 2 for the same two sets of parameters.

We nest discuss the relation between the perturbative and non-perturbative approaches from the point of view of the hadronic models. Here we note their numerical similarity. As shown in Fig. 3, the coupling constant in the perturbative and non-perturbative approaches are close in size for reasonable values of the parameters from very low Q^2 onward ($Q^2 > 0.1$ GeV^2). This result supports the perturbative approach used up to now in model calculations, since it shows, that despite the vicinity of the Landau pole to the hadronic scale, the perturbative expansion is quite convergent and agrees with the non-perturbative results for a wide range of parameters.

3. Non-perturbative Evolution and the Hadron Scale

Let us see how to understand the hadronic scale in the language of models of hadron structure. We use, to clarify the discussion, the original bag model, in its most naive description, consisting of a cavity of perturbative vacuum surrounded by non-perturbative vacuum. The bag model is designed to describe fundamentally static properties, but in QCD all matrix elements must have a scale associated to them as a result of the RGE of the theory. A fundamental step in the development of the use of hadron models for the description of properties at high momentum scales was the assertion that all calculations done in a model should have a RGE scale associated to it [13]. The momentum distribution inside the hadron is only related to the hadronic scale and not to the momentum governing the RG equation. Thus a model calculation only gives a boundary condition for the RG evolution as can be seen for example in the LO evolution equation for the moments of the
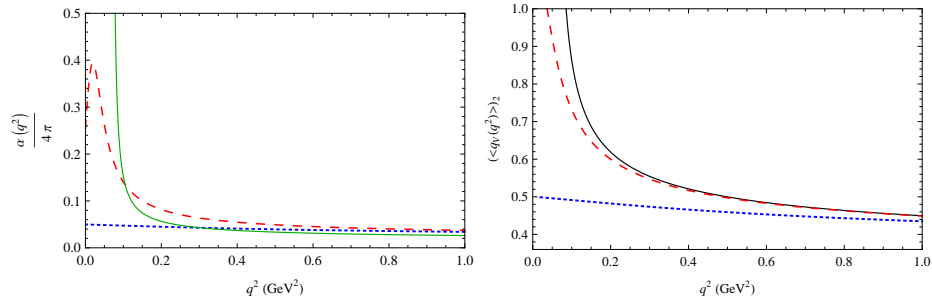
6   *A. Courtoy*

Fig. 3.   Left: The running of the effective coupling. The dotted and dashed curves represent the non-perturbative evolution with the parameters used above. The solid curve shows the NNLO evolution with $\Lambda = 250$ MeV. Right: The evolution of the second moment of the valence quark distribution. The solid curve represents the perturbative LO approximation.

valence quark distribution

$$\langle q_v(Q^2)\rangle_n = \langle q_v(\mu_0^2)\rangle_n \left(\frac{\alpha_s(Q^2)}{\alpha_s(\mu_0^2)}\right)^{d_{NS}^n} , \qquad (6)$$

where d_{NS}^n are the anomalous dimensions of the Non Singlet distributions. Inside, the dynamics described by the model is unaffected by the evolution procedure, and the model provides only the expectation value, $\langle q_v(\mu_0^2)\rangle_n$, which is associated with the hadronic scale. As mentioned in the first Section, the hadronic scale is related to the maximum wavelength at which the structure begins to be unveiled. This explanation goes over to non-perturbative evolution. The non-perturbative solution of the Dyson–Schwinger equations results in the appearence of an infrared cut-off in the form of a gluon mass which determines the finiteness of the coupling constant in the infrared. The crucial statement is that the gluon mass does not affect the dynamics inside the bag, where perturbative physics is operative and therefore our gluons inside will behave as massless. However, this mass will affect the evolution as we have seen in the case of the coupling constant. The generalization of the coupling constant results to the structure function imply that the LO evolution Eq. (6) simply changes by incorporating the non-perturbative coupling constant evolution Eq. (5).

The non-perturbative results, using the same parameters as before, are quite close to those of the perturbative scheme and therefore we are confident that the latter is a very good approximate description. We note however, that the corresponding hadronic scale, for the sets of parameters chosen, turns out to be slightly smaller than in the perturbative case ($\mu_0^2 \sim 0.1$ GeV^2), even for small gluon mass $m_0 \sim 250$ MeV and small $\rho \sim 1$. One could reach a pure valence scenario at higher Q^2 by forcing the parameters but at the price of generating a singularity in the coupling constant in the infrared associated with the specific logarithmic form of

the parametrization. We feel that this strong parametrization dependence and the singularity are non physical since the fineteness of the coupling constant in the infrared is a wishful outcome of the non-perturbative analysis. In this sense, the non-perturbative approach seems to favor a scenario where at the hadronic scale we have not only valence quarks but also gluons and sea quarks [14, 15]. We mean by this statement that to get a scenario with only valence quarks we are forced to very low gluon masses and very small values ρ, while a non trivial scenario allows more freedom in the choice of parameters.

4. Non-perturbative Evolution and Final State Interactions.

The TMDs are the set of functions that depend on both the Bjorken variable x, the intrinsic transverse momentum of the quark $|\vec{k}_\perp|$ as well as on the scale Q^2. The TMDs are fixed by the possible scalar structures allowed by hermiticity, parity and time-reversal invariance. The existence of leading twist final state interactions allows for time-reversal odd functions. Thus by relaxing time-reversal invariance, one defines two additional functions, the Sivers and the Boer-Mulders functions. The growing interest for TMDs called for developments of QCD evolution and its application to PDFs, what has been recently addressed for T-even TMDs in Ref. [16]. Results for T-odd TMDs should follow. In earlier evaluations of T-odd TMDs, the collinear [b] perturbative evolution formalism has been naively applied to describe the behavior of the T-odd Transverse Momentum Dependent parton distribution functions (TMDs) [17, 18, 19].

In the standard approach towards an evaluation of the T-odd distribution functions, the final state interactions are mimicked by a one-gluon-exchange. This gluon exchange is usually described through the inclusion of a perturbative gluon propagator [20, 17]. It is precisely due to this mechanism that these functions have an explicit dependence in the coupling constant and therefore they are ideal to analyze the physical impact of our discussion. Since perturbative QCD governs the dynamics inside the confining region, there is no need to include a non-perturbative massive gluon in the form given by Eq. (4), inside the bag. The main effect of the non-perturbative approach here consists in a change of the hadronic scale μ_0^2 and the value of the running coupling constant at that scale, as clearly illustrated in Fig. 3. This leads to a rescaling of the Sivers and Boer-Mulders functions through a change of $\alpha_s(\mu_0^2)$.

In our previous calculations, we have used the NLO perturbative evolution, with $a(\mu_0^2) \sim 0.1$. Although a solution with this small a can be found, with our choice of parameters, we see, from Fig. 3, that the coupling constant at the hadronic scale in the non-perturbative approach and in the NNLO evolution is consistently larger and lies in the interval $0.1 < a(\mu_0^2) < 0.3$. Taking into account this range we show

---

[b]Collinear, in opposition to transverse, refers to schemes where only longitudinal momenta are relevant. Here: PDFs that depend only on Bjorken-x besides their scale dependence.
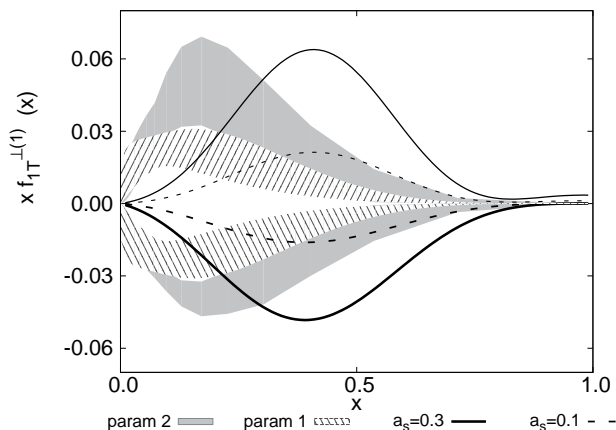
8   *A. Courtoy*

Fig. 4.   The first moment of the Sivers function. The results are given for both the u (thick) and d (normal) distributions. The solid (dashed) curves represent the calculation for $a = 0.3(0.1)$. The bands represent the error band for, respectively, the extraction of the Bochum group (full) and Torino group (stripes).

the first moments of the Sivers function in Fig. 4, where we have two extractions from the data at the SIDIS scale [21, 22]. In order to be able to compare our results to phenomenology, one should apply the QCD evolution equations. If we apply the same band of values of the coupling constant at the hadronic scale to calculation of the Boer-Mulders function we find the results of Fig. 5. We see thus how the naive scenario may serve to predict new observables and determine their experimental feasibility.

The T-odd TMDs have been evaluated in a few models. In most of the models found in the literature final state interactions are approximated by taking into account only the leading contribution due to the one-gluon exchange mechanism. Non-perturbative evaluations of the T-odd functions have been proposed, e.g. non-perturbative eikonal methods [23]. In the latter reference, the authors use a non-perturbative gluon propagator, resulting from a Dyson-Schwinger framework, going therefore beyond one-gluon-exchange approximation by resumming all order contributions. It is worth noticing that the implementation of the final state interactions is model dependent. The discussion we have presented in this paper is not applicable in general to every scheme. The implementation of the non-perturbative evolution as discussed here might be more complex in other (fully non-perturbative) schemes as well as the description of the confinement mechanism.
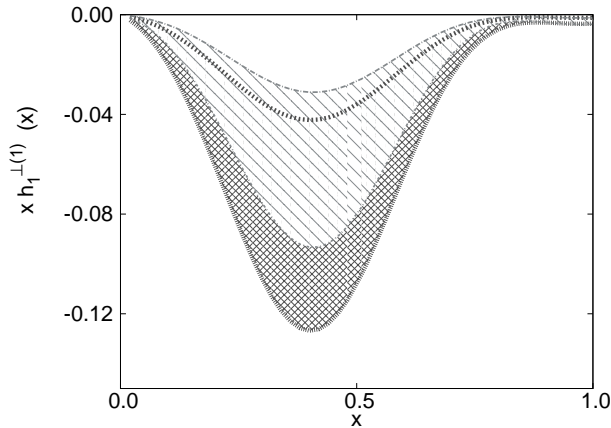
Fig. 5.   The results for the first moment of the Boer-Mulders function calculated within the band $0.1 < a < 0.3$. The results are given for both the u (band between the dotted lines) and d (band with stripes) distributions. Notice that both have the same sign and therefore the bands overlap.

5. Conclusions

The careful analysis of the previous sections shows that the hadronic scale is close to the infrared divergence (Landau pole) of the coupling constant for conventional values of Λ. However, even in this vicinity, the convergence of the $N^m LO$ series is very good for the same Λ and small modifications of it provide an extremely precise agreement for all values of Q^2 to the right of the pole. Moreover, an exciting result is that the values obtained by perturbative QCD with reasonable parameters as defined by DIS data, agree with the non-perturbative evaluation of the coupling constant, which is infrared finite, for parameters which have been chosen to satisfy lattice QCD restrictions of the propagator, with low values of the gluon mass $m_0 \sim$ 250 MeV, and $\rho \sim 1$. The hadronic scale can be interpreted not only from the point of view of perturbative evolution, but also from that of non-perturbative momentum dependence of the coupling constant. Therefore a second result is that the non-perturbative approach provides an explanation of why the evolution from a low hadronic scale, even in the neighbourhood of the Landau pole, is consistent and can be trusted.

It is interesting to see how the non-perturbative framework applies in a simple way to the evaluation of the T-odd TMDs in the bag model. This observation confirms the consistency of our previous calculation within this hadronic model. It enables us to control the physics of the problem from the model side as well as to infer from the evolution scenarios that, as expected, the naive pure valence quark scenario is not favoured. However, it also shows that the naive scenario may well serve to make predictions, within a reasonably small band, which should not be far from experimental expectations.

Like the scale fixing procedure uses experimental data and relies on the knowl-

10   *A. Courtoy*

edge of α_s in the sense of perturbative QCD, vice versa, this new procedure broadens the ways of analyzing the freezing of the running coupling constant: T-odd TMDs are possible candidates to study the behaviour of α_s at intermediate Q^2, following the example of Ref. [24] where the effective coupling constants are phenomenologically extracted.

Acknowledgments

References

1. M. Traini, A. Mair, A. Zambarda and V. Vento, *Nucl. Phys. A* **614**, 472 (1997).
2. M. Stratmann, *Z. Phys. C* **60**, 763-772 (1993).
3. G. Parisi, R. Petronzio, *Phys. Lett. B* **62**, 331 (1976).
4. A. Courtoy, S. Scopetta, V. Vento, *Eur. Phys. J. A* **47**, 49 (2011).
5. J. M. Cornwall, *Phys. Rev. D* **26**, 1453 (1982).
6. A. C. Aguilar and J. Papavassiliou, *JHEP* **0612**, 012 (2006).
7. D. Binosi and J. Papavassiliou, *Phys. Rept.* **479**, 1 (2009).
8. A. C. Aguilar, D. Binosi and J. Papavassiliou, *Phys. Rev. D* **78**, 025010 (2008).
9. C. W. Bernard, *Phys. Lett. B* **108**, 431 (1982).
10. G. Parisi and R. Petronzio, *Phys. Lett. B* **94**, 51 (1980).
11. A. C. Aguilar and J. Papavassiliou, *Eur. Phys. J. A* **35**, 189 (2008).
12. A. C. Aguilar, D. Binosi, J. Papavassiliou and J. Rodriguez-Quintero, *Phys. Rev. D* **80**, 085018 (2009).
13. R. L. Jaffe and G. G. Ross, *Phys. Lett. B* **93**, 313 (1980).
14. S. Scopetta, V. Vento and M. Traini, *Phys. Lett. B* **421**, 64 (1998).
15. S. Scopetta, V. Vento and M. Traini, *Phys. Lett. B* **442**, 28 (1998).
16. S. M. Aybat, T. C. Rogers, *Phys. Rev. D* **83**, 114042 (2011).
17. A. Courtoy, F. Fratini, S. Scopetta and V. Vento, *Phys. Rev. D* **78**, 034002 (2008).
18. A. Courtoy, S. Scopetta and V. Vento, *Phys. Rev. D* **79**, 074001 (2009).
19. A. Courtoy, S. Scopetta and V. Vento, *Phys. Rev. D* **80**, 074032 (2009).
20. F. Yuan, *Phys. Lett. B* **575**, 45 (2003).
21. J. C. Collins, A. V. Efremov, K. Goeke, S. Menzel, A. Metz and P. Schweitzer, *Phys. Rev. D* **73**, 014021 (2006).
22. M. Anselmino *et al.*, *Eur. Phys. J. A* **39**, 89 (2009).
23. L. Gamberg and M. Schlegel, *Phys. Lett. B* **685**, 95 (2010).
24. A. Deur, V. Burkert, J. -P. Chen, W. Korsch, *Phys. Lett. B* **650**, 244-248 (2007).